

# First-principles prediction of a new class of photovoltaic materials: I-III-IV<sub>2</sub>-V<sub>4</sub> phosphides

Jiahong Ma,<sup>1,2</sup> Shiyuan Lin,<sup>2</sup> Guanghan Fan,<sup>1,a)</sup> Guangrui Yao,<sup>1</sup> and Yu-Jun Zhao<sup>2,a)</sup>

<sup>1</sup>*Institute of Optoelectronic Material and Technology, South China Normal University, Guangzhou 510631, People's Republic of China*

<sup>2</sup>*Department of Physics and State Key Laboratory of Luminescent Materials and Devices, South China University of Technology, Guangzhou 510640, People's Republic of China*

(Received 14 March 2012; accepted 9 August 2012; published online 7 September 2012)

A new class of quaternary I-III-IV<sub>2</sub>-V<sub>4</sub>, including CuAlGe<sub>2</sub>P<sub>4</sub>, CuGaGe<sub>2</sub>P<sub>4</sub>, CuAlSn<sub>2</sub>P<sub>4</sub>, and CuGaSn<sub>2</sub>P<sub>4</sub> are studied by density functional theory and beyond for potential photovoltaic application. We found that CuAlGe<sub>2</sub>P<sub>4</sub> and CuGaGe<sub>2</sub>P<sub>4</sub> have a ground state of kesterite (KS) structure, while CuAlSn<sub>2</sub>P<sub>4</sub> and CuGaSn<sub>2</sub>P<sub>4</sub> are nearly energetically degenerated for KS and stannite structures. Interestingly, the band gaps of all the studied quaternary compounds are predicted to be in the range of 1.1–1.7 eV by the hybrid functional calculation and  $\Delta$ -sol approach [M. K.Y. Chan and G. Ceder, *Phys. Rev. Lett.* **105**, 196403 (2010)]. In particular, CuAlSn<sub>2</sub>P<sub>4</sub> in KS structure is predicted to be a potential high-efficiency photovoltaic material since it contains no rare or toxic elements with a direct gap around 1.52 eV. © 2012 American Institute of Physics. [<http://dx.doi.org/10.1063/1.4749421>]

## I. INTRODUCTION

The exploration of high-efficiency materials for the absorber layer of thin film solar cells has attracted great attention these years.<sup>1–8</sup> Nowadays, Si is the widely used in massive manufacture of thin film solar cells because of its mature technology and abundance of material.<sup>1</sup> CdTe could be the runner up with an ideal band gap of 1.45 eV and low cost relative to Si.<sup>1</sup> Cu(In,Ga)Se<sub>2</sub> (CIGS) is another promising material with high efficiency and low cost.<sup>1–3</sup> Cu<sub>2</sub>ZnSnS<sub>4</sub> (CZTS) is the latest hot spot, since it contains only abundant and nontoxic elements with an ideal band gap of about 1.5 eV.<sup>4–8</sup> However, the searching for materials with composite merits of mature technique, high efficiency, low cost, and environment friendliness is still under progress. Hitherto, most of the researches were focused on elements of group IV (IV = Si, Ge), binary compounds of II–VI (II = Zn, Cd, VI = Se, Te) family, ternary and quaternary compounds of I–III–VI<sub>2</sub> (I = Cu, Ag, III = Ga, In, and VI = Se),<sup>1–3,7,9–12</sup> and I–II–IV<sub>2</sub>–VI<sub>4</sub> (I = Cu, Ag, II = Zn, IV = Ge, Sn, and VI = S, Se)<sup>4–8,13</sup> families.

Having similar crystal and electronic structure with binary II–VI compounds, GaAs is also excellent for the development of thin film solar cells with an ideal band gap of 1.43 eV and mature manufacture technology, though the cost is relatively high. Recently, it was reported as the most efficient photovoltaic material with a conversion efficiency of 42.3%.<sup>14</sup>

Likewise, ternary II–IV–V<sub>2</sub> (e.g., ZnGeP<sub>2</sub>),<sup>15</sup> and its extended quaternary I–III–IV<sub>2</sub>–V<sub>4</sub> (e.g., CuAlGe<sub>2</sub>P<sub>4</sub>) compounds could be alternative candidates for solar cells, as they have similar crystal and electronic structure with ternary I–III–VI<sub>2</sub> (e.g., CuInSe<sub>2</sub>) and quaternary I–II–IV<sub>2</sub>–VI<sub>4</sub> (e.g., CuZnSn<sub>2</sub>Se<sub>4</sub>)<sup>4–8,13</sup> ones. However, few reports are found in this aspect, except recent reports on the II–IV–V<sub>2</sub> family of chalcopyrite semiconductors with the formula of

(Mg,Zn,Cd)(Si,Ge,Sn)(P,As)<sub>2</sub>,<sup>15</sup> and II–IV–III<sub>2</sub>–V<sub>4</sub> (e.g., ZnSiAl<sub>2</sub>As<sub>4</sub>, CdGeAl<sub>2</sub>As<sub>4</sub>, and ZnSnGa<sub>2</sub>As<sub>4</sub>).<sup>13</sup>

As high-efficiency materials for solar cells, Si, CdTe, CIGS, CZTS, and GaAs have a common characteristic—an appropriate band gap adapting to the spectrum of solar energy, which is in favor of improving efficiency. In this paper, we have investigated the crystal and electronic structure of some quaternary phosphides (CuAlGe<sub>2</sub>P<sub>4</sub>, CuGaGe<sub>2</sub>P<sub>4</sub>, CuAlSn<sub>2</sub>P<sub>4</sub>, CuGaSn<sub>2</sub>P<sub>4</sub>) constructed through cross substitution<sup>7,8,13,16,17</sup> with first-principles calculations using Perdew-Burke-Ernzerhof (PBE)<sup>18</sup> as well as Heyd-Scuseria-Ernzerhof (HSE)<sup>19</sup> functional. We found that most of their structures, especially kesterite (KS)-CuAlSn<sub>2</sub>P<sub>4</sub>, have potential for materials of high-efficiency solar cells with an appropriate band gap falling in proper range of 1.1–1.7 eV.

## II. COMPUTATION METHODS

We performed the electronic structure and total energy calculations with the plane wave code VASP, applying plane-wave projector augmented-wave (PAW)<sup>20,21</sup> method with PBE exchange correlation functional. An energy cutoff of 400 eV was applied in all the cases. For the Brillouin zone integration, we used symmetrical Monkhorst Pack k-point meshes of 6 × 6 × 4 for a sixteen-atom super cell. We also performed calculation using HSE hybrid functional with energy cutoff of 350 eV, and symmetrical meshes of 5 × 5 × 5 for an eight-atom unit cell. All lattice vectors and atomic positions were fully relaxed by minimizing the quantum mechanical stresses and forces.

Density functional theory (DFT) in the Kohn-Sham implementation<sup>22</sup> with local density approximation (LDA)<sup>22</sup> or generalized gradient approximation (GGA)<sup>23</sup> for the exchange correlation functional, has been successfully applied to structural, electronic, magnetic, and other properties of a myriad of condensed matter systems. However, it fails to correctly predict energy gaps between occupied and

<sup>a)</sup>Authors to whom correspondence should be addressed. Electronic addresses: gfan@scnu.edu.cn and zhaoyj@scut.edu.cn.

unoccupied states referred to as Kohn-Sham gap ( $E_{\text{KS}}$ ), which is a hindrance to researches in fields including semiconductors, optical and photovoltaic materials, and thermoelectrics. Much effort has been devoted to solving this problem through adopting the GW<sup>24</sup> approximation, time dependent DFT,<sup>25</sup> exact exchange,<sup>26</sup> hybrid and screened hybrid functional,<sup>27</sup> or modified Becke-Johnson (MBJ)<sup>28</sup> potentials, but the computational costs are often huge.

$\Delta$ -sol method<sup>29</sup> is an efficient way for predicting band gaps using LDA or GGA functional. It reduces mean absolute errors of band gaps by 70%, compared to Kohn-Sham gaps on over 100 compounds, including II-VI and III-V compounds, with experimental gaps of 0.5–4.0 eV, and the computational costs are similar to typical DFT calculations. In this paper, we use  $\Delta$ -sol method to evaluate band gaps of the desired systems.

The fundamental gap  $E_{\text{FG}}$  of a system is defined as the energy required creating an unbound electron hole pair

$$E_{\text{FG}} = E(N+1) + E(N-1) - 2E(N), \quad (1)$$

where  $N$  is the number of valence electrons in the system. As  $N$  increases, the calculated  $E_{\text{FG}}$  decreases monotonically. The evaluation of  $E_{\text{FG}}$  from Eq. (1) by explicit calculations of energies of the system with  $N$ ,  $N+1$ , and  $N-1$  electrons, produces reasonable results for atoms and molecules, which is referred to as Delta self-consistent-field method ( $\Delta$ SCF).<sup>30</sup> If one takes  $N \rightarrow \infty$  for an infinite solid,  $E_{\text{FG}}$  reverts to  $E_{\text{KS}}$ . If one takes  $N$  as a proper finite number, Eq. (1) can be

applied to solids, which is referred to as  $\Delta$ -sol method. So, the problem is in determining  $N$ . The proper  $N$  is referred to as  $N^* \in [20, 90]$ .<sup>29</sup> The best value of  $N^*$  is determined for each functional such that the mean absolute error between  $E_{\text{FG}}$  and  $E_{\text{exp}}$  across the test set is minimized.

For a system with  $N_0$  valence electrons, to add or remove one per  $N^*$  valence electrons, the number of electrons to add or remove from a unit cell with  $N_0$  valence electrons is  $n = N_0/N^*$ . In most cases,  $n$  is not an integer. We calculate the energies  $E(N_0)$ ,  $E(N_0+n)$ , and  $E(N_0-n)$ , from which we obtain

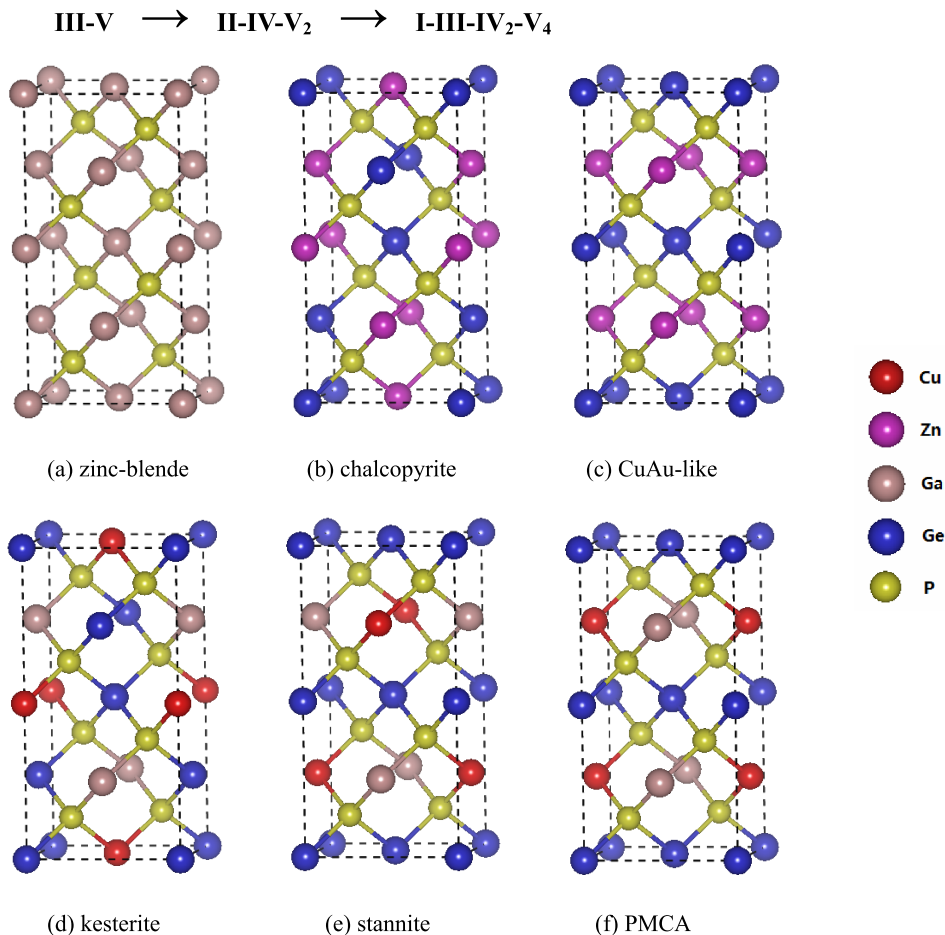
$$E_{\text{FG}} = [E(N_0+n) + E(N_0-n) - 2E(N_0)]/n. \quad (2)$$

We have used the  $\Delta$ -sol method to evaluate band gaps of some sulfides and phosphides, and the results are quite close to available experimental band gaps correspondingly. For example, the  $\Delta$ -sol band gaps of GaP, ZnGeP<sub>2</sub> and ZnSnP<sub>2</sub> are 2.11 eV, 1.85 eV, and 1.77 eV, corresponding to experimental values of 2.35 eV,<sup>31</sup> 2.10 eV,<sup>15</sup> and 1.70 eV,<sup>15</sup> respectively.

### III. RESULTS AND DISCUSSION

#### A. Crystal structures

Binary III-V compounds (e.g. GaP) usually adopt zincblende (ZB) structure [Fig. 1(a)].<sup>31</sup> Through cation cross substitution, ternary II-IV-V<sub>2</sub> compounds (e.g., ZnGeP<sub>2</sub>) can



be constructed by substituting every two group III atoms with one group II and one group IV atom. The substitution gives rise to two completely distinguishing ternary configurations: chalcopyrite (CH) [Fig. 1(b)] and CuAu-like (CA) structure [Fig. 1(c)]. Further, quaternary I-III-IV<sub>2</sub>-V<sub>4</sub> compounds (e.g., CuGaGe<sub>2</sub>P<sub>4</sub>) is generated when the group II cation is replaced by group I and III pairs in ternary II-IV-V<sub>2</sub> compounds. Thereinto, chalcopyrite II-IV-V<sub>2</sub> becomes kesterite (KS) I-III-IV<sub>2</sub>-V<sub>4</sub> [Fig. 1(d)], and CuAu-like II-IV-V<sub>2</sub> give birth to two new quaternary I-III-IV<sub>2</sub>-V<sub>4</sub>: Stannite (ST) [Fig. 1(e)] and the primitive mixed CuAu-like (PMCA) structure [Fig. 1(f)]. PMCA structure has higher total energy than both KS and ST structures and is not considered here.

In contrast to high symmetry III-V ZB structure, ternary II-IV-V<sub>2</sub> compounds require additional parameters to describe their crystal structures besides lattice constant  $a$ : tetragonal lattice distortion parameter<sup>7</sup>  $\eta = c/2a$  and anion displacement parameter<sup>12</sup>

$$u_{\text{CH/CA}} = 0.25 + (R_{\text{II-V}}^2 - R_{\text{IV-V}}^2)/a^2. \quad (3)$$

For quaternary semiconductors, there are four different bonds in KS structure and three in ST structure.<sup>12</sup> As a result, the anion displacement parameters are defined differently

$$u_{\text{KS}} = 0.25 + \left( \frac{R_{\text{I-V}}^2 + R_{\text{III-V}}^2}{2} - \frac{R_{\text{IV1-V}}^2 + R_{\text{IV2-V}}^2}{2} \right) / a^2, \quad (4)$$

$$u_{\text{ST}} = 0.25 + \left( \frac{R_{\text{I-V}}^2 + R_{\text{III-V}}^2}{2} - R_{\text{IV-V}}^2 \right) / a^2. \quad (5)$$

Table I lists the PBE calculated crystal structural parameters. For ZB III-V, tetragonal lattice distortion parameter  $\eta$  equals 1. After atoms of group III are substituted with atoms of group II and group IV, the ZB structure is distorted because the ability of group II atom to bond with group V atom is different from that of group IV atom.<sup>32</sup> In CH structure, the II $\rightarrow$ V $\rightarrow$ IV direction is along the  $a$  or  $b$  axis, while in CA structure, it is along the  $c$  axis. When  $R_{\text{II-V}}$  and  $R_{\text{IV-V}}$  differ, the group V anions will displace from their ideal center and the resulting

TABLE I. Calculated lattice constant  $a$  and  $c$ , tetragonal distortion parameter  $\eta$ , anion displacement parameter  $u$  and its difference between different structures  $\Delta u$ , energy difference  $\Delta E$  (in meV/atom) from PBE calculations.

Structure	$a$ (Å)	$c$ (Å)	$\eta$	$u$	$\Delta u$	$\Delta E$ (meV)
GaP	5.534	11.069	1.000	0.250		0.00
CH-ZnGeP <sub>2</sub>	5.506	10.874	0.987	0.253	0.007	0.00
CA-ZnGeP <sub>2</sub>	5.454	11.071	1.015	0.246		25.64
CA-ZnSnP <sub>2</sub>	5.708	11.441	1.002	0.228	0.001	0.00
CA-ZnSnP <sub>2</sub>	5.718	11.381	0.995	0.227		2.62
KS-CuAlGe <sub>2</sub> P <sub>4</sub>	5.448	10.812	0.992	0.245	0.006	0.00
ST-CuAlGe <sub>2</sub> P <sub>4</sub>	5.416	10.941	1.010	0.239		14.57
KS-CuGaGe <sub>2</sub> P <sub>4</sub>	5.453	10.839	0.994	0.245	0.006	0.00
ST-CuGaGe <sub>2</sub> P <sub>4</sub>	5.432	10.931	1.006	0.239		15.01
KS-CuAlSn <sub>2</sub> P <sub>4</sub>	5.648	11.349	1.005	0.219	0	0.00
ST-CuAlSn <sub>2</sub> P <sub>4</sub>	5.675	11.240	0.990	0.219		-0.43
KS-CuGaSn <sub>2</sub> P <sub>4</sub>	5.661	11.369	1.004	0.220	0	0.00
ST-CuGaSn <sub>2</sub> P <sub>4</sub>	5.682	11.284	0.993	0.220		0.19

cluster is distorted from the ideal tetrahedron, e.g. elongating along the Zn  $\rightarrow$  P  $\rightarrow$  Ge direction, while shrinking in the perpendicular plane. Then the basis vector of CH structure along the  $a$  or  $b$  axis will be longer than those along  $c$  axis, giving  $\eta = 0.987 < 1$  for CH-ZnGeP<sub>2</sub>, while the basis vector of CA structure along  $c$  axis will be longer than those along  $a$  or  $b$  axis, giving  $\eta = 1.015 > 1$  for CA-ZnGeP<sub>2</sub>. For ZnSnP<sub>2</sub>, the radius of Sn is much bigger than that of Zn or Ga. In CH-ZnSnP<sub>2</sub>, the cluster of Zn  $\rightarrow$  P  $\rightarrow$  Sn elongates the basic vector along the  $a$  or  $b$  axis, what is more, the cluster of Sn  $\rightarrow$  P  $\rightarrow$  Sn is along the  $c$  axis, which elongates the basis vector along the  $c$  axis, and the composite effect gives  $\eta = 1.002 > 1$ . In CA-ZnSnP<sub>2</sub>, the cluster of Zn  $\rightarrow$  P  $\rightarrow$  Sn elongates the basic vector along the  $c$  axis, the cluster of Sn  $\rightarrow$  P  $\rightarrow$  Sn elongates the basis vector along the  $a$  or  $b$  axis, and the composite effect gives  $\eta = 0.995 < 1$ .

CuGaGe<sub>2</sub>P<sub>4</sub> and CuGaSn<sub>2</sub>P<sub>4</sub> are derived from ZnGeP<sub>2</sub> and ZnSnP<sub>2</sub> respectively. It is naturally for CuGaGe<sub>2</sub>P<sub>4</sub> and CuGaSn<sub>2</sub>P<sub>4</sub> to follow the trend of ZnGeP<sub>2</sub> and ZnSnP<sub>2</sub> correspondingly. The  $\eta$  of KS and ST structures of CuGaGe<sub>2</sub>P<sub>4</sub> are 0.994 and 1.006, respectively, while they are 1.004 and 0.993 for CuGaSn<sub>2</sub>P<sub>4</sub>. Since the size difference between Ga and Al is not so large (1.81 Å vs. 1.82 Å), the lattice constants change little as Ga is substituted by Al. So CuAlGe<sub>2</sub>P<sub>4</sub> has similar crystal structure with CuGaGe<sub>2</sub>P<sub>4</sub>. Likewise, CuAlSn<sub>2</sub>P<sub>4</sub> also has similar crystal structure with CuGaSn<sub>2</sub>P<sub>4</sub>.

For different structures of the same II-IV-V<sub>2</sub> compound, although they have the same formula, their atom distributions are different, thus, they have different strain energy and Madelung energy, resulting in different total energy. The atom distribution of CH structure is more well-proportioned than CA structure, so CH structure can accommodate the mismatched II-V and IV-V bond lengths with lower strain energy and also lower Madelung energy relative to the CA structure, and generally is adopted as ground state structure.<sup>7</sup> According to the definition of anion displacement parameter  $u$ , it reflects the degree of mismatch of II-V and IV-V bond lengths, and reflects the magnitude of strain energy and Madelung energy. Here we define  $\Delta u$  as the difference of  $u$  between different structures for the moment. In the same compound, the larger  $\Delta u$ , the larger total energy difference  $\Delta E$  per atom. For example,  $\Delta u$  of ZnGeP<sub>2</sub> is 0.007 and the corresponding  $\Delta E$  is 25.64 meV, while  $\Delta u$  of ZnSnP<sub>2</sub> is only 0.001 and  $\Delta E$  is only 2.62 meV. Though the conclusion above is not strict, it reflects the truth to a certain extent, also for quaternary phosphides. The calculated  $\Delta u$  of both CuAlGe<sub>2</sub>P<sub>4</sub> and CuGaGe<sub>2</sub>P<sub>4</sub> are 0.006, and the corresponding  $\Delta E$  are 14.57 and 15.01 meV.  $\Delta u$  of both CuAlSn<sub>2</sub>P<sub>4</sub> and CuGaSn<sub>2</sub>P<sub>4</sub> are zero, as their  $\Delta E$  are very small, only 0.43 and 0.19 meV, respectively.

Table II lists the crystal results calculated from HSE functional. To save time, we only calculated the quaternary phosphides here. The lattice constants  $a$  and  $c$  from HSE calculations are a little smaller than those from PBE. This could be ascribed to the fact that HSE functional has stronger  $sp$  coupling<sup>8,19</sup> with results of shorter  $R_{\text{III-V}}$  and  $R_{\text{IV-V}}$ , thus, with larger  $u$ . Take KS-CuAlSn<sub>2</sub>P<sub>4</sub> as an example,  $R_{\text{III-V}}$  and  $R_{\text{IV-V}}$  from HSE are 2.381 and 2.525 Å, respectively, correspondingly those from PBE are 2.401 and 2.560 Å,  $u$  from HSE is 0.223 and the corresponding  $u$  from PBE is 0.219.

TABLE II. Calculated lattice constant  $a$  and  $c$ , tetragonal distortion parameter  $\eta$ , anion displacement parameter  $u$  and its difference between different structures  $\Delta u$ , as well as the energy difference  $\Delta E$  (in meV/atom) from HSE calculation.

Structure	$a$ (Å)	$c$ (Å)	$\eta$	$u$	$\Delta u$	$\Delta E$ (meV)
KS-CuAlGe <sub>2</sub> P <sub>4</sub>	5.404	10.695	0.990	0.249	0.006	0.00
ST-CuAlGe <sub>2</sub> P <sub>4</sub>	5.359	10.873	1.014	0.243		18.19
KS-CuGaGe <sub>2</sub> P <sub>4</sub>	5.407	10.720	0.991	0.249	0.006	0.00
ST-CuGaGe <sub>2</sub> P <sub>4</sub>	5.370	10.853	1.011	0.243		18.14
KS-CuAlSn <sub>2</sub> P <sub>4</sub>	5.603	11.260	1.005	0.223	0	0.00
ST-CuAlSn <sub>2</sub> P <sub>4</sub>	5.633	11.136	0.989	0.223		-1.43
KS-CuGaSn <sub>2</sub> P <sub>4</sub>	5.611	11.259	1.003	0.223	0	0.00
ST-CuGaSn <sub>2</sub> P <sub>4</sub>	5.634	11.167	0.991	0.223		-1.05

However, the structural parameters from HSE are compatible with those from PBE on the whole, testifying each other the reliability of results.

## B. Electronic structures

The calculated band gaps of CuAlGe<sub>2</sub>P<sub>4</sub>, CuGaGe<sub>2</sub>P<sub>4</sub>, CuAlSn<sub>2</sub>P<sub>4</sub>, and CuGaSn<sub>2</sub>P<sub>4</sub> are listed in Table III, which indicates that the values from the  $\Delta$ -sol method and HSE approach are quite consistent with each other, with a difference within 0.3 eV. We found that the band gaps of CuAlGe<sub>2</sub>P<sub>4</sub>, CuGaGe<sub>2</sub>P<sub>4</sub>, CuAlSn<sub>2</sub>P<sub>4</sub>, and CuGaSn<sub>2</sub>P<sub>4</sub> fall into the range of 1.1–1.7 eV from  $\Delta$ -sol method except ST-CuAlGe<sub>2</sub>P<sub>4</sub>, and ST-CuGaGe<sub>2</sub>P<sub>4</sub>, and so for those from HSE calculations except ST-CuGaSn<sub>2</sub>P<sub>4</sub>. Furthermore, we calculated their band structures with HSE functional. We found that KS-CuAlSn<sub>2</sub>P<sub>4</sub> and KS-CuGaSn<sub>2</sub>P<sub>4</sub> possess direct gaps (c.f. Table III), while the other studied systems have indirect gaps from our HSE calculated band structures, which is shown in Fig. 2 exemplified with KS-CuAlSn<sub>2</sub>P<sub>4</sub>. According to our results, all the four quaternary phosphides have appropriate band gaps for high-efficiency solar cells. In particular, KS-CuAlSn<sub>2</sub>P<sub>4</sub> could be the most promising one, for it has a direct gap (1.34 eV for  $\Delta$ -sol and 1.52 eV for HSE) close to GaAs and contains no rare and toxic elements as CZTS. Further experimental exploration for KS-CuAlSn<sub>2</sub>P<sub>4</sub> is suggested for a new high-efficiency photovoltaic material.

To understand the electronic structure of the studied compounds, we also calculated the density of states (DOS) from both PBE and HSE functionals. Take KS-CuAlSn<sub>2</sub>P<sub>4</sub> as

TABLE III. Anion displacement parameter with PBE  $u^{\text{PBE}}$ , energy gap with  $\Delta$ -sol  $E_g^{\Delta\text{-sol}}$ , anion displacement parameter with HSE  $u^{\text{HSE}}$ , energy gap with HSE  $E_g^{\text{HSE}}$  and direct-gap or not.

Structure	$u^{\text{PBE}}$	$E_g^{\Delta\text{-sol}}$ (eV)	$u^{\text{HSE}}$	$E_g^{\text{HSE}}$ (eV)	Direct-gap
KS-CuAlGe <sub>2</sub> P <sub>4</sub>	0.245	1.41	0.249	1.63	No
ST-CuAlGe <sub>2</sub> P <sub>4</sub>	0.239	1.05	0.243	0.85	no
KS-CuGaGe <sub>2</sub> P <sub>4</sub>	0.245	1.38	0.249	1.36	no
ST-CuGaGe <sub>2</sub> P <sub>4</sub>	0.239	1.03	0.243	0.73	No
KS-CuAlSn <sub>2</sub> P <sub>4</sub>	0.219	1.34	0.223	1.52	yes
ST-CuAlSn <sub>2</sub> P <sub>4</sub>	0.219	1.25	0.223	1.18	no
KS-CuGaSn <sub>2</sub> P <sub>4</sub>	0.220	1.28	0.223	1.18	yes
ST-CuGaSn <sub>2</sub> P <sub>4</sub>	0.220	1.24	0.223	1.02	no

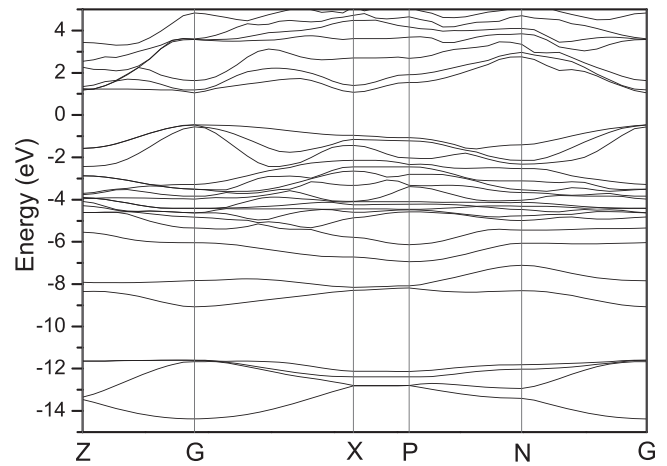


FIG. 2. Band structure of KS-CuAlSn<sub>2</sub>P<sub>4</sub> from HSE calculation.

an example (c.f. Fig. 3). In the tetragonal crystal field, the  $d$  states of Cu are divided into doubly degenerated  $e$  orbitals and triply degenerated  $t_2$  orbitals. The  $e$  states do not participate in bonding with P, and their DOS is localized [Fig. 3(a)]. The  $t_2$  states hybridize with the  $p$  states of P, and their DOS has two peaks, corresponding to bonding and anti-bonding states [Fig. 3(a)]. The  $d$  levels of Cu are higher than the  $s$  level of Sn and Al, so the top of valence bands is mainly made up of anti-bonding states of Cu  $t_2$  states and P  $p$  states [Figs. 3(a) and 3(d)]. The  $s$  states of Sn hybridize with the  $p$  states of P, divided into bonding states (about from  $-13$  to  $-10$  eV) [Fig. 3(b)] and anti-bonding states (about from 0.5 to 2.0 eV) [Fig. 3(b)]. The bottom of conduction bands is mainly composed of anti-bonding states of Sn  $s$  states and P  $p$  states [Figs. 3(b) and 3(d)]. The  $s$  levels of Al are higher than those of Sn and have little proportion at the bottom of conduction bands. Fig. 4 shows the DOS of KS-CuAlSn<sub>2</sub>P<sub>4</sub> with HSE, it is similar to that with PBE.

According to the analysis above, we conclude for quaternary phosphides: the top of valence bands is mainly composed of the anti-bonding  $d$  orbitals of Cu and  $p$  orbitals of P.

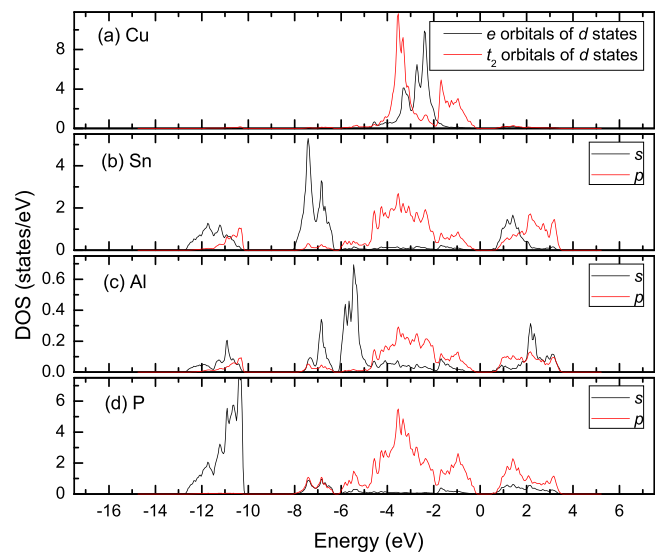


FIG. 3. Projected DOS of KS-CuAlSn<sub>2</sub>P<sub>4</sub> with PBE, (a)  $d$  states of Cu, (b)  $s$  and  $p$  states of Sn, (c)  $s$  and  $p$  states of Al, (d)  $s$  and  $p$  states of P.

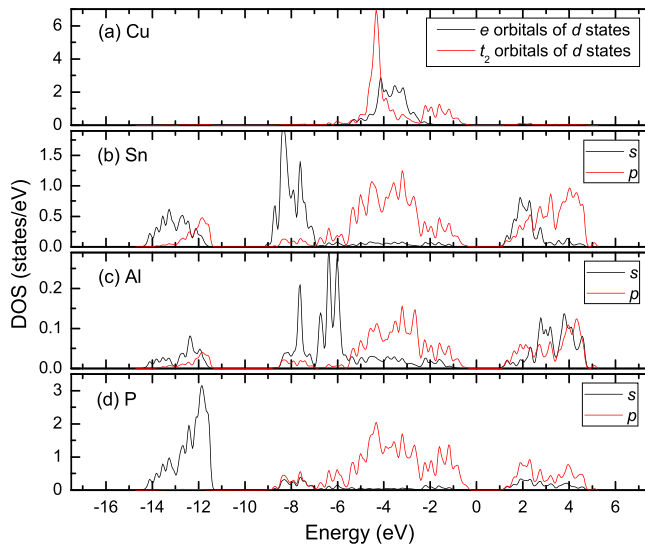


FIG. 4. Projected DOS of KS-CuAlSn<sub>2</sub>P<sub>4</sub> with HSE, (a) *d* states of Cu, (b) *s* and *p* states of Sn, (c) *s* and *p* states of Al, (d) *s* and *p* states of P.

Stronger *pd* hybridization, often accompanied with smaller bond length of Cu-P and smaller anion displacement parameter *u*, results in smaller band gap. The bottom of conduction bands is mainly composed of the anti-bonding *s* orbitals of Sn and *p* orbitals of P. Stronger *sp* hybridization, often accompanied with smaller bond length of IV-P and larger anion displacement parameter *u*, results in larger band gap. Therefore, KS structure generally has larger band gap than ST structure, because KS structure has weaker *pd* coupling and stronger *sp* coupling. In the same compound, the anion displacement parameter *u* of KS structure is generally larger than that of ST structure. It is consistent for both  $\Delta$ -sol method and HSE calculations. As listed in Table III, KS-CuAlGe<sub>2</sub>P<sub>4</sub> has a larger *u* of 0.249 with a larger band gap of 1.63 eV, while ST-CuAlGe<sub>2</sub>P<sub>4</sub> has a smaller *u* of 0.243 with a smaller band gap of 0.85 eV from HSE calculations.

As we pointed out that the band gaps of all the studied I-III-IV<sub>2</sub>-VI<sub>4</sub> compounds are predicted to be in the range of 1.1–1.7 eV by the hybrid functional calculation and  $\Delta$ -sol approach. In particular, CuAlSn<sub>2</sub>P<sub>4</sub> in KS structure is predicted to be with a direct gap around 1.52 eV, close to the reported experimental band gap of Cu<sub>2</sub>ZnSnS<sub>4</sub> (1.5 eV). While Cu<sub>2</sub>ZnSnS<sub>4</sub> is stabilized at KS structure, CuAlSn<sub>2</sub>P<sub>4</sub> is nearly energetically degenerated at KS and ST structures with ST structure lowered by 3 meV/f.u. We believe that CuAlSn<sub>2</sub>P<sub>4</sub> is promising for photovoltaic material as Cu<sub>2</sub>ZnSnS<sub>4</sub> did, and it is worthwhile for the experimentalists to give it a shot.

#### IV. CONCLUSION

Structural and electronic properties of a new class of quaternary I-III-IV<sub>2</sub>-V<sub>4</sub>, including CuAlGe<sub>2</sub>P<sub>4</sub>, CuGaGe<sub>2</sub>P<sub>4</sub>, CuAlSn<sub>2</sub>P<sub>4</sub>, and CuAlSn<sub>2</sub>P<sub>4</sub> are investigated by PBE and HSE calculations. It is found that CuAlSn<sub>2</sub>P<sub>4</sub> and CuGaSn<sub>2</sub>P<sub>4</sub> are nearly energetically degenerated for their KS and ST structures, while CuAlGe<sub>2</sub>P<sub>4</sub> and CuGaGe<sub>2</sub>P<sub>4</sub> in KS structure are

energetically favored. The band gaps of the quaternary compounds are predicted to be in the range of 1.1–1.7 eV by the hybrid functional calculation and  $\Delta$ -sol approach. We predicted that KS-CuAlSn<sub>2</sub>P<sub>4</sub> is a potential high-efficiency photovoltaic material since it contains no rare or toxic elements with a direct gap around 1.52 eV, and suggested further experimental exploration.

#### ACKNOWLEDGMENTS

This work is supported by the National Natural Science Foundations of China (61176043, 11174082), Fund for Strategic and Emerging Industries of Guangdong Province (2010A081002005), and Cooperation Project in Industry, University and Institution of Guangdong province and Ministry of Education of People's Republic of China (2010B090400192).

- <sup>1</sup>K. L. Chopra, P. D. Paulson, and V. Dutta, *Prog. Photovoltaics* **12**, 69 (2004).
- <sup>2</sup>M. A. Contreras, B. Egaas, K. Ramanathan, J. Hiltner, A. Swartzlander, F. Hasoon, and R. Noufi, *Prog. Photovoltaics* **7**, 311 (1999).
- <sup>3</sup>M. A. Contreras, K. Ramanathan, J. A. Shama, F. Hasoon, D. L. Young, B. Egass, and R. Noufi, *Prog. Photovoltaics* **13**, 209 (2005).
- <sup>4</sup>J.-S. Seol, S.-Y. Lee, J.-C. Lee, H.-D. Nam, and K.-H. Kim, *Sol. Energy Mater. Sol. Cells* **75**, 155 (2003).
- <sup>5</sup>J. J. Scragg, P. J. Dale, and L. M. Peter, *Electrochem. Commun.* **10**, 639 (2008).
- <sup>6</sup>S. Chen, X. G. Gong, A. Walsh, and S.-H. Wei, *Appl. Phys. Lett.* **94**, 041903 (2009).
- <sup>7</sup>S. Chen, X. G. Gong, A. Walsh, and S.-H. Wei, *Phys. Rev. B* **79**, 165211 (2009).
- <sup>8</sup>J. Paier, R. Asahi, A. Nagoya, and G. Kresse, *Phys. Rev. B* **79**, 115126 (2009).
- <sup>9</sup>S. B. Zhang, S.-H. Wei, and A. Zunger, *Phys. Rev. Lett.* **78**, 4059 (1997).
- <sup>10</sup>S. B. Zhang, S.-H. Wei, and A. Zunger, *Phys. Rev. B* **57**, 9642 (1998).
- <sup>11</sup>S.-H. Wei and S. B. Zhang, *J. Phys. Chem. Solids* **66**, 1994 (2005).
- <sup>12</sup>Y. Zhang, X. Yuan, X. Sun, B.-C. Shih, P. Zhang, and W. Zhang, *Phys. Rev. B* **84**, 075127 (2011).
- <sup>13</sup>S. Chen, W.-J. Yin, J.-H. Yang, X. G. Gong, A. Walsh, and S.-H. Wei, *Appl. Phys. Lett.* **95**, 052102 (2009).
- <sup>14</sup>A. Luque, *J. Appl. Phys.* **110**, 031301 (2011).
- <sup>15</sup>M. V. Schilfgaarde, T. J. Coutts, N. Newman, and T. Peshek, *Appl. Phys. Lett.* **96**, 143503 (2010).
- <sup>16</sup>C. H. L. Goodman, *J. Phys. Chem. Solids* **6**, 305 (1958).
- <sup>17</sup>B. R. Pamplin, *J. Phys. Chem. Solids* **25**, 675 (1964).
- <sup>18</sup>J. P. Perdew, K. Burke, and M. Ernzerhof, *Phys. Rev. Lett.* **77**, 3865 (1996).
- <sup>19</sup>J. Heyd, G. E. Scuseria, and M. Ernzerhof, *J. Chem. Phys.* **118**, 8207 (2003).
- <sup>20</sup>P. E. Blöchl, *Phys. Rev. B* **50**, 17953 (1994).
- <sup>21</sup>G. Kresse and D. Joubert, *Phys. Rev. B* **59**, 1758 (1999).
- <sup>22</sup>W. Kohn and L. J. Sham, *Phys. Rev.* **140**, A1133 (1965).
- <sup>23</sup>D. C. Langreth and J. P. Perdew, *Phys. Rev. B* **21**, 5469 (1980).
- <sup>24</sup>L. Hedin, *Phys. Rev.* **139**, A796 (1965).
- <sup>25</sup>E. Runge and E. K. U. Gross, *Phys. Rev. Lett.* **52**, 997 (1984).
- <sup>26</sup>M. Städele, M. Moukara, J. A. Majewski, P. Vogl, and A. Görling, *Phys. Rev. B* **59**, 10031 (1999).
- <sup>27</sup>A. D. Becke, *J. Chem. Phys.* **98**, 5648 (1993); C. Lee, W. Yang, and R. G. Parr, *Phys. Rev. B* **37**, 785 (1988); J. P. Perdew, M. Ernzerhof, and K. Burke, *J. Chem. Phys.* **105**, 9982 (1996); A. V. Krukau et al., *ibid.* **125**, 224106 (2006).
- <sup>28</sup>F. Tran and P. Blaha, *Phys. Rev. Lett.* **102**, 226401 (2009).
- <sup>29</sup>M. K.-Y. Chan and G. Ceder, *Phys. Rev. Lett.* **105**, 196403 (2010).
- <sup>30</sup>R. M. Martin, *Electronic Structure: Basic Theory and Practical Methods* (Cambridge University Press, Cambridge, England, 2004).
- <sup>31</sup>R. Ahmed, Fazal-e-Aleem, S. J. Hashemifar, and H. Akbarzadeh, *Physica B* **403**, 1876 (2008).
- <sup>32</sup>J. E. Jaffe and A. Zunger, *Phys. Rev. B* **29**, 1882 (1984).